Absorption Spectra of First-Row Transition Metal Complexes of Bacteriochlorins: A Theoretical Analysis

Laurence Petit,[†,‡] Carlo Adamo,[‡] and Nino Russo*[,†]

Dipartimento di Chimica and Centro di Calcolo ad Alte Prestazioni per Elaborazioni Parallele e Distribuite Centro d'Eccellenza MURST - Università della Calabria, I-87030 Arcavacata di Rende, Italy, and Laboratoire d'Électrochimie et de Chimie Analytique, CNRS UMR-7575, École Nationale Supérieure de Chimie de Paris (ENSCP), 11 rue P. et M. Curie, F-75231 Paris Cedex 05, France

Received: February 7, 2005; In Final Form: April 27, 2005

A theoretical study on a family of divalent transition metal bacteriochlorin complexes (M−BC, where M = Mn, Fe, Co, Ni Cu, and Zn) has been carried out to elucidate their potentialities as active molecules in photodynamic therapy (PDT). To draw a complete picture of their electronic properties, both for the ground and excited states, these complexes have been studied by the means of density functional theory (DFT). The time-dependent DFT (TDDFT) approach was used to interpret the electronic spectra, while solvent effects were taken into account by explicitly considering both two water molecules coordinated to the central metal atom and the contribution from the solvent bulk. Particular attention has been devoted to the analysis of the so-called Q bands, since these can be particularly important for medical applications. Metal substitution and environment (solvent) effects have been analyzed, and good agreement is found between computed and available UV−vis spectra. These theoretical data, especially those relative to the metallobacteriochlorins not yet completely characterized at the experimental level, could give some hints for future medical applications.

1. Introduction

Since 1900, when Raab discovered the destroying power of light on bioorganisms,[1] the use of photochemistry in biology and medicine has been greatly developed, and nowadays, the so-called photodynamic therapy (PDT) is an efficient way to treat different diseases in oncology and ophthalmology.[2−4] The basic principle[5] is to inject into the blood a photosensitizing agent that is gathered into cells. When these cells are irradiated with a source of light of the appropriate wavelength, usually a laser, the photosensitizer can be activated and the energy is then transferred to nearby molecules via a radiationless transition. In particular, triplet molecular oxygen ($^3O_2$) can be excited into the singlet state that is cytotoxic and can then destroy nearby cells, for example, cancerous cells. With the required excitation energy being quite low, about 1 eV (around 1300 nm), it can be easily obtained through several photosensitizers. Among them, metal derivatives of porphine-like macrocycles are currently used in clinical applications.[6,7] The interesting property of such molecules is their absorption bands in visible light, called Q bands. The red light is indeed necessary, since the light penetration into tissues depends exponentially on the wavelength.

Free base bacteriochlorin (FBBC, Figure 1), which derivates from porphyrin by the reduction of two outer double bonds, is particularly worthwhile, since it presents, among other bands, a stronger and red shifted absorption maximum around 710 nm.[5] In this perspective, numerous experimental works have been devoted to the synthesis of new substituted bacteriochlorins designed for their absorption at high wavelengths. Recently, Fukuzumi et al.[8] have succeeded in modifying the bacteriochlorin ring so as to add up Q bands as high as 800 nm.

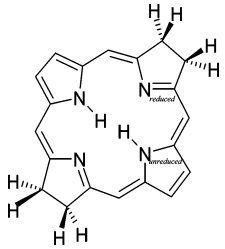

Figure 1. Sketch of the structure of free basebacteriochlorin (FBBC) and atom labeling.

Similarly, within the past two decades, metal octaethylisobacteriochlorins (OEiBCs) have been extensively studied as models for prosthetic groups involved in biochemical cycles of carbon, nitrogen, and sulfur (Ni(II) OEiBC for the cofactor F430 of methylreductases[9,10] and Cu(II) OEiBC and Fe(II) OEiBC for the sirohydrochlorin in nitrite and sulfite reductases[11,12]). In this way, as for metalloporphyrins, it has been established that complexation with transition metals could modify the optical properties of such a molecule.[13−15] Still, to our knowledge, few theoretical works have been dedicated to the study of metallobacteriochlorins, with the exception of free base bacteriochlorin,[16−20] and complexes with zinc and magnesium.[17,21] To explore the potentialities of these complexes as effective substitutes for the current photoactive molecules, we have undertaken a systematic theoretical study on the structural and electronic properties of a family of metal(II) bacteriochlorin complexes (M−BC, where M = Mn, Fe, Co, Ni, Cu, and Zn). In particular, we have carried out density functional theory (DFT) calculations both on isolated and solvated molecules in water. The influence of the solvent was examined using a supramolecular approach in order to explicitly simulate the effect of the first solvation shell of the metal atom, while the bulk solvent effect has been introduced through a polarizable

* Corresponding author. E-mail: nrusso@unical.it.
† Università della Calabria.
‡ ENSCP.

10.1021/jp050667d CCC: $30.25
Published on Web 05/25/2005

continuum model.[22] Next, excited state properties have been evaluated by the time-dependent extension of DFT to the calculation of excited states[23] that provides an accurate description of UV−vis transitions of metal-containing systems (see, for instance, refs 24 and 25). Our ultimate purpose is to highlight the interesting help that theoretical calculations can bring in designing new photosensitizers.

2. Computational Methods

All calculations were performed at the density functional level of theory with the hybrid functional PBE0.[26] This functional is based on the generalized gradient functional PBE (Perdew−Burke−Ernzerhof)[27] with 25% exact exchange. Some tests were nevertheless made with the B3LYP hybrid functional, which has only 20% Hartree−Fock exchange,[28] as well as with the PW91 GGA functional.[29,30] Restricted formalism was used for closed shell systems, and unrestricted formalism was used otherwise. In this last case, spin contamination, monitored by the expectation value of S^2, was found to be negligible for any considered spin state. All calculations were carried out with the Gaussian 03 package.[31]

All the structures were optimized with the 6-31G(d) basis set for all atoms except the metal which was described by the pseudopotential LANL2DZ and its corresponding valence basis set.[32,33] Such a level of theory has been successfully applied in a number of papers concerning the structure, spectroscopic properties, and reactivity of several tetrapyrroles[34,35] and more generally of organometallic systems.[24,25,36]

As for free base bacteriochlorin (FBBC), the D_{2h} symmetry was imposed for all M−BC complexes, whereas, for complexes with explicit water molecules, we made use of C_{2v} symmetry. Yet, we previously checked that ruffling distortions reported in several papers[35,37] were negligible by relaxing geometries.

Absorption spectra were computed as vertical excitations from the minima of the ground state structures using the time-dependent DFT (TDDFT) approach as implemented in Gaussian.[38] Here, different basis sets have been considered for metal atoms, namely, the all-electron DZVP[39] and 6-311+G(d)[40] basis sets as well as the LANL2DZ pseudopotential, while the 6-31+G(d) basis set was used for all the other atoms.

Solvent effects were evaluated using the conductor-like approach within the framework of the polarizable continuum model (PCM).[22,41] This approach provides results very close to those obtained by the original dielectric model for high dielectric constant solvents, but it is significantly more effective in geometry optimizations and less prone to numerical errors arising from the small part of the solute electron cloud lying outside the cavity (escaped charge effects). Solvent shifts of excitation bands were evaluated by a recent nonequilibrium implementation[42] of the polarizable continuum model.

Finally, the electronic structure of these molecules has been investigated using the natural bond orbital (NBO) approach and the related natural population analysis (NPA).[43] The NPA approach is also particularly effective for inorganic complexes, since it gives a description of the electronic distribution that is less sensitive to the computational parameters (e.g., basis set).

3. Results and Discussion

3.1. Ground State Properties. Owing to the few available data on M−BC, the first step in our investigation was to determine the ground and the lowest excited electronic states. This point is of particular relevance for the use of M−BC in PDT, as the lowest excited electronic state of the photosensitizer activates the molecular oxygen from its ground triplet to the singlet state. Since the energy difference of the two states in O_2 is about 1 eV, the energy difference of two electronic states in M−BC must be at least equal to this gap.

TABLE 1: Total (hartrees) and Relative Energies (eV) for All of the Considered Bacteriochlorin Complexes with and without the Two Water Molecules Coordinated to the Metal Atom

molecule	molecular symmetry	electronic state	total energy	ΔE
Isolated Systems				
Mn−BC	D_{2h}	$^4B_{3u}$	−1093.6069	0.56
Mn−BC	D_{2h}	^6A_g	−1093.6277	0
Fe−BC	D_{2h}	$^3B_{3g}$	−1113.1061	0
Fe−BC	D_{2h}	^5A_u	−1113.0671	1.06
Co−BC	D_{2h}	^2A_g	−1134.7377	0
Co−BC	D_{2h}	^4A	−1134.6924	0.27
Ni−BC	D_{2h}	^1A_g	−1158.9510	0
Ni−BC	D_{2h}	^3A_u	−1158.9280	0.63
Cu−BC	D_{2h}	^2A_g	−1185.7743	0
Cu−BC	D_{2h}	$^4B_{2u}$	−1185.7404	0.92
Zn−BC	D_{2h}	^1A_g	−1055.1501	0
Zn−BC	D_{2h}	$^3B_{2u}$	−1055.1153	0.95
Cluster with Two Water Molecules				
Mn−BC−2H_2O	C_{2v}	$^2B_1$	−1246.2633	1.47
Mn−BC−2H_2O	C_{2v}	$^6A_1$	−1246.3175	0
Fe−BC−2H_2O	C_{2v}	$^1A_1$	−1265.7786	0.33
Fe−BC−2H_2O	C_{2v}	$^3B_1$	−1265.7909	0
Co−BC−2H2O	C_{2v}	$^2A_1$	−1287.4219	0
Co−BC−2H2O	C_{2v}	$^4A_1$	−1287.3850	1.00
Ni−BC−2H_2O	C_{2v}	$^3A_1$	−1311.6526	0
Ni−BC−2H_2O	C_{2v}	$^1A_1$	−1311.6207	0.87
Cu−BC−2H_2O	C_{2v}	$^2A_1$	−1338.4501	0
Cu−BC−2H_2O	C_{2v}	$^4A_1$	−1338.4148	0.96
Zn−BC−2H_2O	C_{2v}	$^1A_1$	−1207.8389	0
Zn−BC−2H_2O	C_{2v}	$^3A_1$	−1207.8031	0.97

This task is not trivial, as demonstrated by the large amount of works devoted to this aspect for related metalloporphyrins.[43,50] This is exemplified by the correct assignment of triplet ground state to the iron(II) porphyrin complex which was a difficult challenge both at experimental and theoretical levels.[46,47,50−54] To better assess this point, we have considered the lowest spin states for each complex, chosen on the basis of the experimental data, except for Zn(II)−BC and Cu(II)−BC for which there is no ambiguity on their ground electronic states. We have selected several multiplicities for each complex among those of lowest energy, as reported for metalloporphyrins.[43,50] The total and relative energies of the two most stable states are catalogued in Table 1. For the Mn−BC complex, doublet, quartet, and sextet spin states have been considered: the last one has been characterized as the ground state, while the two others ($^2B_{1g}$ and $^4B_{3u}$) are about 1.6 and 0.6 eV higher in energy, respectively. A high spin state has also been found for Fe−BC ($^3B_{3g}$). In contrast, the ground states of all the other metal complexes correspond to the lowest spin multiplicity: doublet for Co and Cu complexes and singlet for Ni and Zn ones. For these complexes, the low-lying excited states lie high in energy, with the gap ranging between 0.3 and 0.6 eV.

As a general trend, we remark that our results are consistent with previous works on porphyrin.[43−54] Nevertheless, the ground state of both cobalt(II) and nickel(II) porphyrin is still under discussion, since recent studies, at the SDCI level of theory, suggest the quartet and the triplet, respectively, as the lowest states,[48,49] in contrast with related experiments.[55−57] Therefore, to double check our results, we have compared different functionals and basis sets. The B3LYP exchange-correlation functional in conjunction with the LANL2DZ, DZVP, and 6-31++G(d,p) pseudopotential or all-electron basis sets always indicates that the singlet is the ground state, with the energy

TABLE 2: Distances (Å) of the Metal−Nitrogen Bond for Bacteriochlorin Complexes[a]

complex	$d(M-N_{unreduced\ pyrrole})$	$d(M-N_{reduced\ pyrrole})$	$d(M-O_{H_2O})$
FBBC	2.091	2.122	
Mn−BC	2.054	2.161	
	(2.086)	(2.168)	(2.433)
Fe−BC	1.984	2.049	
	(2.013)	(2.052)	(2.397)
Co−BC	1.980	2.039	
	(1.992)	(2.062)	(2.356)
Ni−BC	1.963	2.029	
	(2.041)	(2.118)	(2.208)
Cu−BC	2.023	2.154	
	(2.010)	(2.108)	(2.604)
Zn−BC	2.028	2.143	
	(2.061)	(2.151)	(2.338)

[a] The corresponding experimental values for Zn−BC are 2.043 and 2.122 Å.[46] In parentheses are reported the values computed for the complex with two water molecules.

gap ranging between 0.47 eV (B3LYP/LANL2DZ) and 1.03 eV (B3LYP/DZVP). Likewise, the PW91 functional with the LANL2DZ pseudopotential for the metal give the singlet 0.86 eV lower than the triplet.

We have to also notice that only the Co complex has an energy gap between the ground and the excited state slightly larger than the singlet/triplet splitting in molecular oxygen.

From a geometrical point of view, the free base bacteriochlorin cavity is larger than the porphyrin one. Indeed, the β hydrogenation of two opposite pyrroles results in an increase of the C−N−C angle between the corresponding nitrogens and the carbons in the meso position.

The enlargement of the central hole might prevent major deformations from planarity.[58,59] Yet, several X-ray structures of different kinds of tetrapyrroles display ruffling distortions of the metal.[35,37] To verify this point, we have relaxed all of the geometrical parameters, allowing for out-of-plane motion of the metal atoms and of the macrocycle. In any case, a planar rearrangement has been found and the D_{2h} symmetry was thus kept for FBBC and the M−BC complexes.

At the same time, due to the reduction of pyrroles, the corresponding nitrogens are pulled away from the cavity center. The complexation does not modify this trend, leading to two classes of M−N distances. All of these distances are listed in Table 2: they flicker between 1.963 and 2.027 Å for the unreduced pyrroles and between 2.028 and 2.160 Å for the reduced pyrroles (see Figure 1). The distances to unreduced pyrroles in M−BC are rougthly the same as those for metalloporphyrins.[60,61] In contrast, the distances to reduced pyrroles are longer, with a mean increase of 0.09 Å. Unlike the evolution of ionic radii, these values slightly fall in going from Mn to Ni and thereafter they rise again until Zn. This could suggest a stronger bonding interaction for metal from Fe to Ni relative to Mn, Cu, and Zn. Since the geometry of Zn−BC is available in the literature,[62] a comparison between the X-ray structure and our theoretical calculations is possible. There is a general good agreement between the two structures, especially for the macrocyle parameters, where the differences do not exceed the experimental error. A slight discrepancy is found for the metal−nitrogen distances, with the deviation being around 0.02 Å.

Atomic charge analysis performed at the NBO level can give additional information about the interaction between the transition metal and the bacteriochlorin ligand. In all examined compounds, we found the same charge distribution behavior arranged in five concentric circles whose charge alternates from one circle to the next one. Starting from a positive charge on the metal center, a first negative shell that includes the four pyrrole nitrogens is present. The two carbon-type rings that follow are respectively positive and negative. Eventually, the last ring is positively charged and includes all hydrogen atoms. Since all metals have a formal oxidation number of +II, their lower charge is consistent with a slightly covalent interaction with the nitrogens of the ligand. From Table 3 emerges that zinc is the metal that has the lowest interaction with the ligand while the strongest one is with nickel. All the information coming from charge distribution analysis is consistent with the corresponding general shape found in the literature for metalated porphyrins.[48]

TABLE 3: NPA Charges (au) for the M(II)−Bacteriochlorin Complexes, Computed for the Bare System or Complexed with Two Water Molecules and Embedded in a Continuum Solvent

	Mn	Fe	Co	Ni	Cu	Zn
Gas Phase						
metal	1.55	1.14	1.13	1.01	1.32	1.68
$N_{reduced}$	−0.75	−0.66	−0.63	−0.61	−0.69	−0.78
$N_{unreduced}$	−0.63	−0.54	−0.54	−0.52	−0.58	−0.65
porphine-like cycle	−1.55	−1.14	−1.13	−1.01	−1.32	−1.68
Cluster with Two Water Molecules and Continuum						
metal	1.52	0.84	1.09	1.38	1.33	1.69
$N_{reduced}$	−0.72	−0.57	−0.62	−0.68	−0.69	−0.75
$N_{unreduced}$	−0.63	−0.51	−0.55	−0.61	−0.60	−0.65
porphine-like cycle	−1.61	−1.16	−1.20	−1.52	−1.38	−1.75
H_2O	0.05	0.16	0.05	0.07	0.03	0.03

To better understand how each metal interacts with bacteriochlorin, we must keep in mind that the greatest bonding interaction is between the metal d_{x2-y2} orbital, lying in the molecular plane, and the nitrogen orbitals with the appropriate symmetry. The strongest interaction is calculated for Fe, Co, and Ni. A NBO analysis of the d_{x2-y2} occupation within the molecular complexes gives a population in the order of 1 e^- for Ni−BC and of about 0.6 e^- for Fe−BC and Co−BC. Their d_{x2-y2} level should be, in principle, empty, and our result well undelines the donation from the nitrogen doublets. It is therefore not surprising that these metals bear the lowest positive charges (see Table 3) and shortest distances to nitrogens. In contrast, the weakest interactions are found for d^5 Mn and d^{10} Zn, with these atoms having the d_{x2-y2} orbital half-filled and completely filled, respectively. Here, the NPA electronic populations are 1 and 2 e^-, as expected. Eventually, Cu shows an intermediate behavior, since the d_{x2-y2} orbital has an occupation of 1.4 e^-, that is, an excess of 0.4 e^- with respect to a formal d^9 population. Once again, the computed distances and charges well underline these trends.

This metal−ligand bonding is furthermore strengthened by weaker π interactions between the d_π orbitals of the metal and the p orbitals of nitrogens. All these interactions are stabilizing and energetically low, so these orbitals are not directly involved in the electronic excitations falling in the UV range.

3.2. Spectrochemical Behavior. As a first step, we have computed the electronic spectrum of the Zn−BC complex, since the presence in the literature of both experimental and theoretical data allows us to validate the use of the TDDFT procedure. It is well-known that the spectroscopic behavior of porphyrin-like complexes can be rougthly rationalized in terms of the Gouterman four-orbital model, where the principal excitations involve the two highest occupied molecular orbitals (HOMO and next-HOMO) and the two lowest unoccupied orbitals (LUMO and next-LUMO).[63]

A first check was made on the chosen functional PBE0 with respect to the widely used B3LYP functional using the same

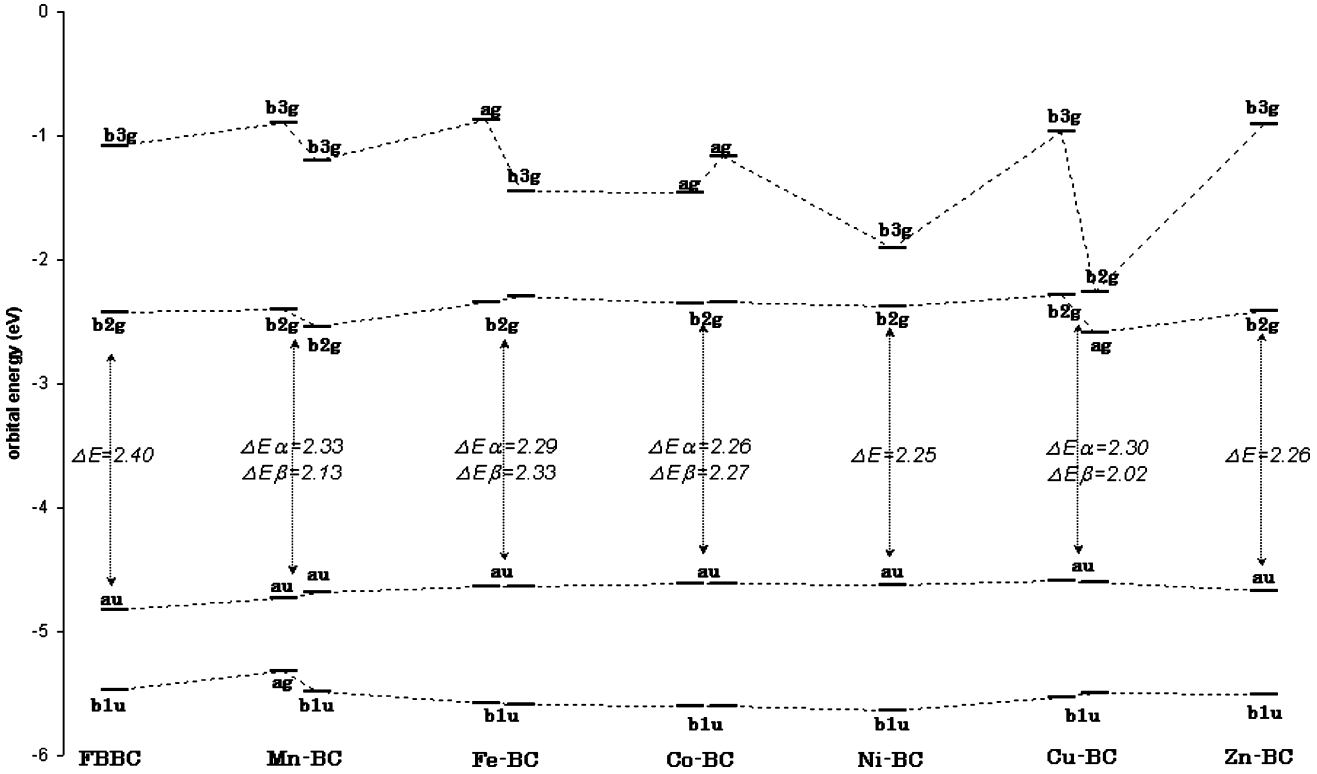

Figure 2. Orbital energy levels for the four Gouterman orbitals of metal(II)−BC.

basis sets (LANL2DZ for zinc and 6-31+G(d) for other atoms). The results are very close, with a mean difference of less than 0.05 eV for transitions and 0.01 for oscillator strengths. Then, we checked the basis sets for both metal and ligand atoms. Concerning the metal, the efficiencies of the LANL2DZ pseudopotential and the TZVP and 6-311+G(d) all-electron basis sets were compared, whereas the remaining atoms (carbon, hydrogen, and nitrogen) were each time described with the 6-31+G(d) basis set. For both Q*x* and Q*y* bands, the three basis sets give results that differ from each other by about 2 nm and 0.001 for intensities. For bacteriochlorin atoms, the results are similar with the 6-31+G(d) and 6-31++G(2d) basis sets. All the other computations were thereby performed with the PBE0 functional coupled with the LANL2DZ pseudopotential for the metal center and the 6-31+G(d) basis set for the remaining atoms.

By and large, our calculations match well with previous theoretical works[17,64] and experiments on the zinc tetraphenylbacteriochlorin-pyridine.[62] These are the only experimental data on a metallobacteriochlorin complex belonging to our series, and we will thus focus our analysis on the Zn−BC system. The Q*y* band of Zn−BC (2.56 eV) is quite close to the experimental value (2.20 eV) and in good agreement with previously reported TDDFT results (2.44 eV), performed with Slater orbitals and a gradient corrected functional.[17] At the same time, excellent agreement is found with the value computed at a sophisticated post-Hartree−Fock level (2.54 eV), namely, the multireference perturbation theory (MRPT) model.[63] For the Q*x* band, our work and the previous DFT study[17] give a value of 2.04 eV that is 0.4 eV higher than the experimental counterpart while the MRPT value is closer to experiments (1.56 vs 1.65 eV). A similar discrepancy has already been reported in the literature[17] and has been attributed to an unsuitable description of the virtual orbitals involved in the excitations. All the same, this discrepancy is in the range expected for TDDFT calculations.[24,65] It is nonetheless assumed that the substituents of the experimental complex can shift wavelengths upward, thus contributing for a part to the observed discrepancy.[37] One can also note that all our values tend to overestimate the excitation energy. The same trend is observed for B bands: we calculated them to be at 3.68 eV (B*y*) and 3.81 eV (B*x*), whereas experiments report respective values of 3.20 and 3.46 eV.[62] These bands are nonetheless not implied in phototherapy processes, so we do not analyze herein this part of the spectrum. Depending on the complex, the relative intensity of the two B bands can change.

TABLE 4: Energies (eV) and Oscillator Strengths (in Parentheses) for the Q Bands of M(II)−Bacteriochlorin Complexes

complex	Q*x* band	Q*y* band	B*y* band	B*x* band
FBBC	2.10 (0.24)	2.57 (0.05)	3.81 (1.14)	4.10 (1.11)
Mn−BC	1.99 (0.25)	2.46 (0.05)	3.49 (0.51)	3.94 (0.49)
Fe−BC	2.05 (0.26)	2.62 (0.01)	3.09 (0.15)	3.93 (0.63)
Co−BC	2.04 (0.28)	2.66 (0.03)	3.72 (0.55)	3.83 (0.26)
Ni−BC	2.02 (0.26)	2.65 (0.03)	3.69 (0.61)	3.82 (0.10)
Cu−BC	2.05 (0.25)	2.58 (0.01)	3.57 (0.63)	3.77 (0.25)
Zn−BC	2.04 (0.27)	2.56 (0.04)	3.68 (0.18)	3.81 (0.88)

Absorption spectra of octaethylisobacteriochlorin (OEiBC) complexes of other metals, such as cobalt, nickel, and copper, have also been studied by Stolzenberg et al.[13,37,66] However, this ligand significantly differs from the presently analyzed bacteriochlorin by ethyl susbtituents on pyrroles and, more important, by the position of reduced double bonds localized on two successive pyrroles. It is thus expected that their excitation energies differ from those for our bacteriochlorins. As matters stand, discrepancies with experimental OEiBC complexes are akin to the one for Zn−BC. The only exception is the Q*x* band that is markedly lower, leading to a smaller discrepancy in the order of a hundredth of an electronvolt.[66]

All the computed vertical transitions are collected in Table 4. Analyzing this table, we can observe that the metalation process causes respectively red shifting and blue shifting of Q*x* and Q*y* bands with respect to the free base bacteriochlorin. These effects occur for all of the systems, with the exception of the

Q*y* band of the Mn complex that is slightly red shifted. Note that red shifting is also observed for metal OEiBC complexes, in comparison with the bare *trans*-OEiBC.[66] As expected from the Gouterman four-orbital model,[63] the Q*x* band arises mainly from the HOMO → LUMO transition (around 60% on average) with a contribution from the next-HOMO → next-LUMO excitation (about 40%). The Q*y* band is equally composed of next-HOMO → LUMO and HOMO → next-LUMO excitations. Figure 2 shows the relative energies of such orbitals for each metal complex (directly involved in the excitation process) as well as the corresponding orbitals for FBBC. The first point to underline is the regular aspect of this diagram. No drastic change appears in comparison with FBBC even if the HOMO → LUMO gap energy is on average 0.13 eV lower than that for the isolated ligand. The presence of the metal atom seems to slightly strengthen the relaxation of degeneracy of FBBC thanks to the interaction with the ligand. As for porphyrins,[53] the metal has little influence on the gap and thus on Q bands. To explain Q band values, one should keep in mind the main configuration of each band mentioned before. As expected, the highest transition corresponds to free base bacteriochlorin that has the highest gap (2.40 eV). For the other systems, we must consider both alpha and beta gap energies and their corresponding percentages. For instance, the iron Q*x* band is composed of 44% of the beta HOMO → LUMO transition and 40% of the alpha one; that is, the mean gap is approximately 2.31 eV. In this way, it is easy to rationalize all of the transition energies for Q*x* bands. When the gap energy is similar, the difference between next-HOMO and next-LUMO must then be compared.

Moving to intensities, we can note that they slightly step up in M−BC relative to FBBC. Figure 3 displays the four Gouterman orbitals for Zn(II)−BC and Fe(II)−BC. These two complexes are indeed the most representative of the two kinds of orbitals that can be found along the series. In particular, the iron complex presents two orbitals with a metal character, with the d_{x2-y2} orbital being involved in the next-LUMO (Figure 3, right). It must be noticed that when the metal character is negligible, α and β levels are almost degenerate, as is almost the case for next-HOMO and HOMO. On the contrary, significant metal character is noted for LUMO and next-LUMO, so these orbitals are energetically different. The other metallobacteriochlorins have a similar behavior, with the exception of zinc. In this particular case, no metal character is observed in the four frontier orbitals, whatever the level is.

3.3. Environmental Effects: The Role of the Solvent. The main interest in metal bacteriochlorin complexes lies in their possibility to be used in PDT, and therefore, these systems should be stable enough in aqueous solution and preserve their properties in biological media.[67] Consequently, a theoretical analysis considering the interaction with the solvent can give better insight on their working mechanisms.

The influence of water molecules on electronic properties may be considered in two ways: explicitly, by adding few water molecules around the complex, or implicitly, using a continuum solvent model.[22] The first approach is mandatory, since solvent molecules (e.g., water) are often directly coordinated to the metal center in order to complete its coordination sphere. At the same time, the reaction field generated by the interaction with the bulk solvent could significantly modulate the electronic distribution of the solute, thus affecting its spectral properties.[68] As recently demonstrated, solvent continuum models well reproduce UV−vis spectra in solution, notably when coupled with a discrete explicit treatment of the solvent molecules strongly bound to the solute.[69]

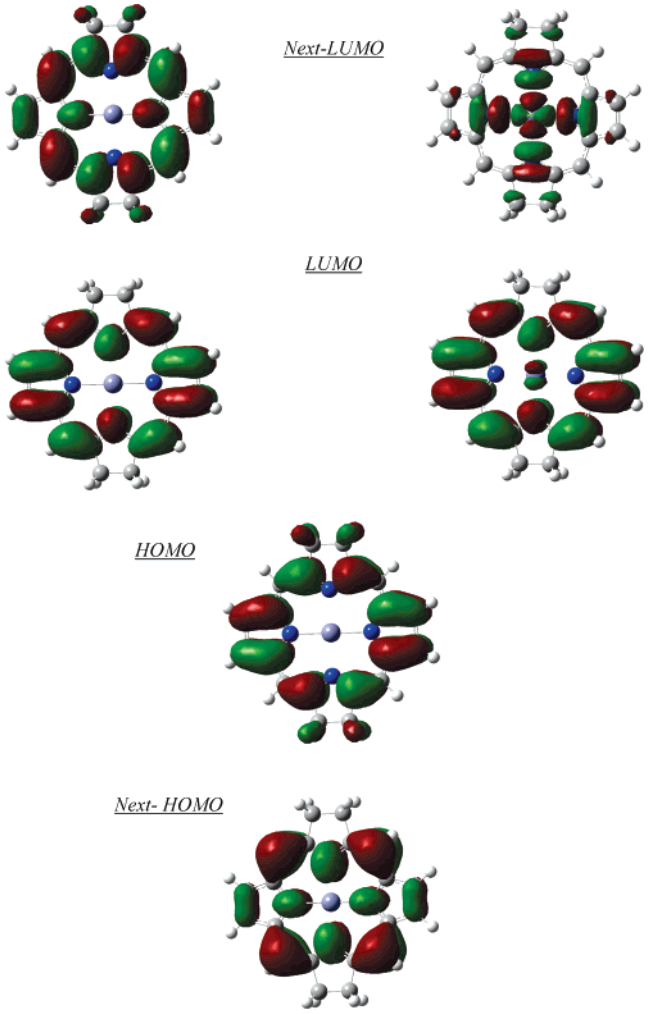

Figure 3. Plot of the four Gouterman orbitals for zinc(II) bacteriochlorin (Zn−BC, on the left) and iron(II) bacteriochlorin (Fe(II)−BC, on the right). Next-HOMO and HOMO are similar for both complexes. The corresponding orbitals of the other metal(II) bacteriochlorin complexes resemble those of iron greatly.

As a first step, we have considered two water molecules to complete the coordination sphere of the metal, thus reaching an octahedral topology. Previous experimental works often report a coordination number of 5 or 6 with solvent molecules such as pyridine or piperidine.[14,37] Full geometry optimizations have been performed on both ground and low-lying excited states, since the change in coordination could affect the relative energies. The only exceptions are the Cu and Zn complexes for which the assignment of the ground state can be evaluated on the basis of trivial chemical evidence ($^2A_1$ and $^1A_1$, respectively). The results are collected in Table 1. The ligand field of the two added water molecules does not change the spin state of the M−BC complexes, except for the Ni, for which the hexa-coordinated system has a triplet ground state (see Table 1). This last result is consistent with the literature data on Ni(II) porphyrins[41] and Ni(II) octaethylisobacteriochlorin with two pyridines.[14,37]

More interesting, the two water molecules significantly increase the energy difference between the different spin states. The net effect is that upon coordination all the complexes have an energy gap close to 1 eV, with the only exception being the Fe−BC complex. Since in a biological environment this situation is highly probable, these molecules fulfill one of the main requirements needed to be used as PDT agents.

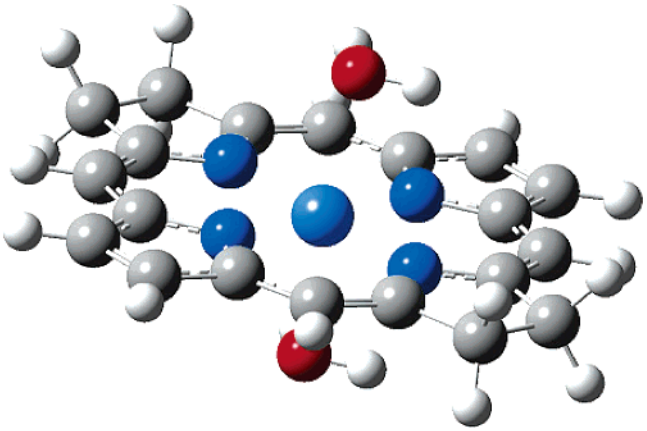

Figure 4. Optimized geometry of the Co(II) bacteriochlorin complex with two water molecules, in C_{2v} symmetry.

The C_{2v} optimized geometry of the Co(II)−BC complex with two water molecules is given in Figure 4. As for bare complexes, geometries were relaxed so as to test whether ruffling distortions could occur. No important change from C_{2v} symmetry was nonetheless observed. Table 2 sums up the main structural parameters. Very small changes are found in comparison with the bond lengths obtained for the bare molecules. We can nonetheless notice a mean increase of 0.04 Å for the distance to unreduced pyrroles. This aspect is slightly strengthened for the Ni(II)−BC + $2H_2O$ complex. The distances to unreduced and reduced pyrroles are respectively 0.08 and 0.09 Å longer than those in the gaseous phase, whereas the distance to water is the lowest. All the same, the absolute mean distance to water molecules remains quite high (2.39 Å).

To clarify this qualitative aspect, we have calculated binding energies between the M−BC complex and solvent molecules. All the values have been corrected for the effects related to the basis set superposition error.[70] The obtained values are −16.3 kcal/mol (Mn−BC), −7.3 kcal/mol (Fe−BC), −12.4 kcal/mol (Co−BC), −29.1 kcal/mol (Ni−BC), −7.3 kcal/mol (Cu−BC), and −15.8 kcal/mol (Zn−BC). These energies well correlate the axial M−O distances (Table 2). These results are consistent with an interaction between water and a metal center, always stronger than a typical H-bond interaction between two water molecules (about 5.0 kcal/mol[71]). This rough estimate suggests that in aqueous solution the metal is always hexacoordinated.

Water molecules have a small effect on the electronic distribution of M−BC, as can be seen from the data collected in Table 3. A small transfer (less than 0.1 $|e^-|$) from the water to the metal is observed which does not change when adding the solvent reaction field.

TABLE 5: Energies (eV) and Oscillator Strengths (in Parentheses) for the Q Bands of Metal(II)−Bacteriochlorin Complexes Computed with Two Water Molecules and Bulk Solvent (CPCM)[a]

complex	Q*x* band	Δ*E*	Q*y* band	Δ*E*
FBBC−CPCM	2.01 (0.36)	−0.09	2.55 (0.09)	−0.02
Mn−BC−$2H_2O$	2.04 (0.25)	0.05	2.42 (0.06)	−0.04
Mn−BC−$2H_2O$−CPCM	1.94 (0.38)	−0.05	2.39 (0.11)	−0.07
Fe−BC−$2H_2O$	2.08 (0.25)	0.03	2.58 (0.03)	−0.04
Fe−BC−$2H_2O$−CPCM	1.98 (0.38)	−0.07	2.57 (0.06)	−0.05
Co−BC−$2H_2O$	2.07 (0.26)	0.03	2.57 (0.04)	−0.09
Co−BC−$2H_2O$−CPCM	1.96 (0.38)	−0.08	2.56 (0.08)	−0.10
Ni−BC−$2H_2O$	2.07 (0.27)	0.05	2.49 (0.05)	−0.16
Ni−BC−$2H_2O$−CPCM	1.97 (0.40)	−0.05	2.47 (0.10)	−0.18
Cu−BC−$2H_2O$	2.04 (0.25)	−0.01	2.53 (0.04)	−0.05
Cu−BC−$2H_2O$−CPCM	1.94 (0.37)	−0.11	2.52 (0.08)	−0.06
Zn−BC−$2H_2O$	2.07 (0.27)	0.03	2.46 (0.05)	−0.10
Zn−BC−$2H_2O$−CPCM	1.96 (0.40)	−0.08	2.44 (0.11)	−0.12
Zn−BC−CPCM	1.97 (0.40)	−0.07	2.52 (0.10)	−0.04

[a] The computed shifts (Δ*E*, eV) with respect to the corresponding system in the gas phase are also reported.

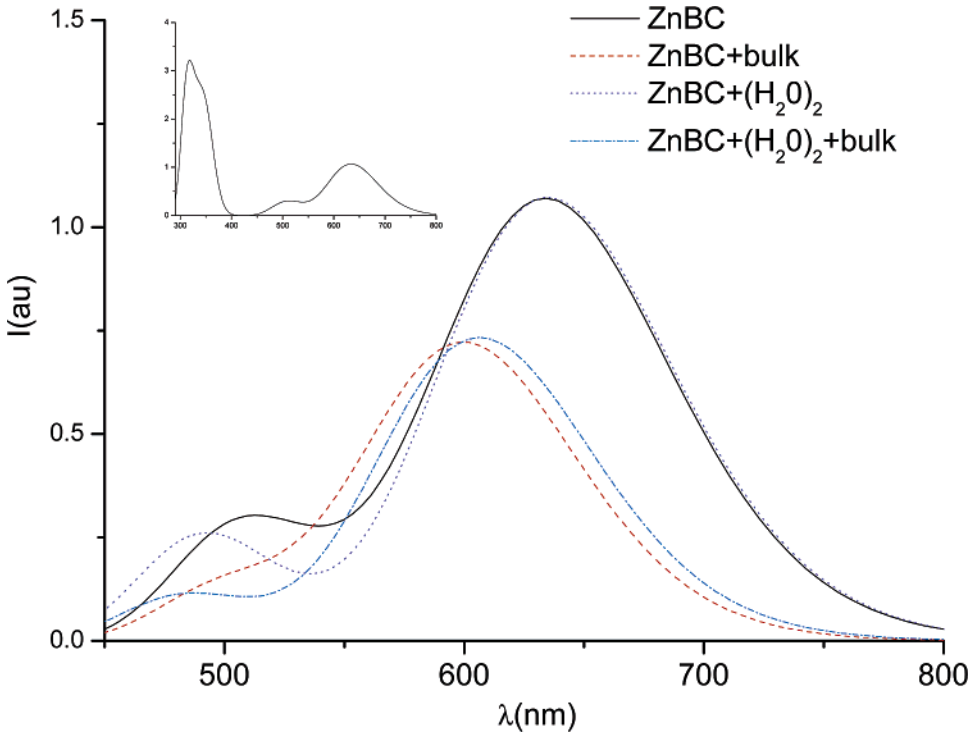

Figure 5. Computed UV spectra (Q bands) for the Zn(II) bacteriochlorin complex both in the gas phase or in solution (bulk) and with or without two water molecules. The spectra are reproduced by associating a single Gaussian function, with a broadening of 0.15 eV, to each computed transition and normalizing the absorbance to 1. In the inset is reported the complete spectra of the Zn(II) bacteriochlorin complex with two water molecules.

Nevertheless, there are two noteworthy exceptions. First, for Ni, the solvent induces significant electron redistribution from the metal to BC, so that the positive charge on Ni is almost 0.4 $|e^-|$ higher. Second, an opposite effect is observed for Fe, where the charge is about 0.3 $|e^-|$ lower than that in the gas phase.

This weak interaction between water and the metal center slightly affects the UV spectra. In Table 5 are reported the vertical electronic transitions computed for the water complexes, either isolated or embedded in the continuum solvent. Note that the B bands are not deeply affected by solvent effects and are thus not reported in the table. From these data, it is evident that the coordinated water molecules blue shift the Q*x* band of about 0.03 eV with respect to the gas phase, with the only exception being the copper complex, which is slightly red shifted (about 0.01 eV). The Q*y* band is shifted upward (about 0.04 eV) in all of the complexes. The addition of the bulk solvent via the continuum model results in a general and significant increase of the wavelengths. This effect is particularly relevant for the Q*x* band where the red shift with respect to the bare water complex assumes values of almost 40 nm. However, since the effects of bulk and explicit solvents are opposite, the total variations with respect to the M−BC complex are smaller (about 0.1 eV), as can be seen from the shifts reported in Table 5. Q*x* bands are thus greatly enhanced when adding the solvent reaction field. In contrast, there is little influence of the solvent on Q*y* bands, with the red shift being of a few nanometers with respect to the water complex. We must also notice the strong influence of the bulk solvent on the oscillator strengths of all transitions and, therefore, on intensities.

To decouple the two effects (explicit water molecules vs bulk), we have evaluated how the bulk solvent influences the UV spectra in the case of Zn−BC as well as for the free ligand (see Table 5). In both cases, a red shift of about 0.07 eV has been found for the Q*x* band, while a lower variation occurs for the Q*y* band. The overall effects of the solvent on the UV spectrum of Zn−BC are well represented in the plot of Figure 5.

A brief energetic comparison of the frontier orbitals with and without the solvent reaction field reveals a global stabilization of the four Gouterman orbitals. These levels involve orbitals on nitrogens that are easily polarized and are thus stabilized by the solvent.

The frontier orbital picture is quite similar to what was found in a vacuum, since not only are the gap energies almost the same but also HOMO and LUMO are globally at the same energy levels. Nevertheless, the next-HOMO and next-LUMO orbitals are destabilized in the presence of the two water molecules. The composition of orbitals backs up this result: whereas HOMO and LUMO have mainly a ligand character, metal dπ orbitals and contributions from the water oxygens appear in next-HOMO and next-LUMO. Therefore, solvent effects on the Q*y* bands have an orbital origin, whereas the red shifts of the Q*x* transitions are merely due to polarization effects.

4. Conclusion

In the present paper, we have worked out in detail, using a DFT approach, the properties of metal(II) bacteriochlorins both in the gas phase and in aqueous solution. Different electronic states, geometrical parameters, population analyses, and excited states have been computed, analyzed, and compared. Careful attention was given to the upper part of the electronic spectra (Q bands), since our ultimate goal was a better knowledge of the potential advantages of metallobacteriochlorins for photodynamic therapy. In this perspective, the influence of the solvent is studied: explicit water molecules as axial ligands do not highly interact with the metal, and excitations are consequently slightly affected. On the other hand, the inclusion of bulk effects, by a polarizable dielectric continuum, improves the results significantly, since Q*x* bands are red shifted and the oscillator strength is increased.

Besides the spectrochemical behavior, all the considered systems, with the exception of the iron complex, have in solvent an energy gap between the low and high spin states of about 1 eV, taking into account a reasonable error bar for our similations ($\pm$0.3 eV). Since this is a fundamental requirement to activate molecular oxygen, these molecules could fulfill also another criterion for photodynamic therapy applications.

In conclusion, we hope that our data, especially for the metalated bacteriochlorins not yet completely characterized at the experimental level, will help the experimental chemists in finding some indications for the future use in medical applications of metal(II) bacteriochlorins.

Acknowledgment. N.R. thanks Università della Calabria and Regione Calabria (POR) for the financial support. C.A. and L.P. are grateful to CNRS for financial support in the framework of the ACI "Jeune Équipe 2002" project and to the French National Computer Center (IDRIS) for a generous grant of computer time (project 41703). L.P. also wishes to thank Università della Calabria for a grant and the kind hospitality shown to her while being a visitor.

References and Notes

(1) Raab, O. *Z. Biol.* **1900**, *39*, 524−546.
(2) Sessler, J. L.; Hemmi, G.; Mody, T. D.; Murai, T.; Burrell, A.; Young, S. W. *Acc. Chem. Res.* **1994**, *27*, 43.
(3) Hajri, A.; Wack, S.; Meyer, C.; Smith, M. K.; Leberquier, M.; Aprahamian, M. *Photochem. Photobiol.* **2002**, *75*, 140−148.
(4) Van Tenten, Y.; Schuitmaker, H. J.; De Wolf, A.; Willekens, B.; Vrensen, G. F. J. M.; Tassignon, M. J. *Exp. Eye Res.* **2001**, *72*, 41−48.
(5) MacDonald, I. J.; Dougherty, T. J. *J. Porphyrins Phthalocyanines* **2001**, *5*, 105−129.
(6) Rosenthal, D. I.; Nurenberg, P.; Becerra, C. R.; Frenkel, E. P.; Carbone, D. P.; Lum, B. L.; Miller, R.; Engel, J.; Young, S.; Miles, D.; Renschler, M. F.; *Clin. Cancer Res.* **1945**, *5*, 739.
(7) Rockson, S. G.; Kramer, P.; Razavi, M.; Szuba, A.; Filardo, S.; Adelman, D. C. *Circulation* **2000**, *102*, 2322.
(8) Fukuzumi, S.; Ohkubo, K.; Chen, Y.; Pandey, R. K.; Zhan, R.; Shao, J.; Kadish, K. M. *J. Phys. Chem. A* **2002**, *106*, 5105−5113.
(9) Pfaltz, A.; Jaun, B.; Fassler, A.; Eschenmoser, A.; Jaenchen, R.; Gilles, H. H.; Deikert, G.; Thauer, R. K. *Helv. Chim. Acta* **1982**, *65*, 828.
(10) Ellefson, W. L.; Whitman, W. B.; Wolf, R. S. *Proc. Natl. Acad. Sci. U.S.A.* **1982**, *79*, 3707.
(11) Murphy, M. J.; Siegel, L. M.; Tover, S. R.; Kamin, H. *Proc. Natl. Acad. Sci. U.S.A.* **1974**, *71*, 612.
(12) Vega, J. M.; Kamin, H. *J. Biol. Chem.* **1977**, *252*, 892.
(13) Stolzenberg, A. M.; Schussel, L. J. *Inorg. Chem.* **1991**, *30*, 3205−3213.
(14) Renner, M. W.; Furenlid, L. R.; Stolzenberg, A. M. *J. Am. Chem. Soc.* **1995**, *117*, 293−300.
(15) Huang, W.-Y.; Wild, U. P.; Johnson, L. W. *J. Phys. Chem.* **1992**, *96*, 6189−6195.
(16) Parusel, A. B. J.; Grimme, S. *J. Porphyrins Phthalocyanines* **2001**, *5*, 225−232.
(17) Yamaguchi, Y.; Yokoyama, S.; Mashiko, S. *J. Chem. Phys.* **2002**, *116*, 6541−6548.
(18) Hasegawa, J.; Ozeki, Y.; Ohkawa, K.; Hada, M.; Nakatsuji, H. *J. Phys. Chem. B* **1998**, *102*, 1320−1326.
(19) Parusel, A. B. J.; Ghosh, A. *J. Phys. Chem. A* **2000**, *104*, 2504−2507.
(20) Kuzmitsky, V. A.; et al. *Chem. Phys.* **2004**, *298*, 1−16.
(21) Linnanto, J.; Korppi-Tommola, J. *J. Phys. Chem. A* **2001**, *105*, 3855−3866.
(22) Tomasi, J.; Persico, M. *Chem. Rev.* **1994**, *94*, 2027.
(23) Casida, M. E. In *Recent Advances in Density Functional Methods, Part I*; Chong, D. P., Ed.; World Scientific: Singapore, 1995.
(24) Ciofini, I.; Lainé, P. P.; Bedioui, F.; Adamo, C. *J. Am. Chem. Soc.* **2004**, *126*, 10763.

(25) Ciofini, I.; Daul, C.; Adamo, C. *J. Phys. Chem. A* **2003**, *107*, 11182.
(26) Adamo, C.; Barone, V. *J. Chem. Phys*. **1999**, *110*, 6158.
(27) Perdew, J. P.; Burke, K.; Ernzerhof, M. *Phys. Rev. Lett*. **1996**, *77*, 3865; **1997**, *78*, 1396.
(28) Becke, A. D. *J. Chem. Phys*. **1993**, *98*, 5648.
(29) Becke, A. D. *Phys. Rev. A* **1988**, *38*, 3098.
(30) Perdew, J. P. *Phys. Rev. B* **1986**, *33*, 8822.
(31) Frisch, M. J.; Trucks, G. W.; Schlegel, H. B.; Scuseria, G. E.; Robb, M. A.; Cheeseman, J. R.; Montgomery, J. A., Jr.; Vreven, T.; Kudin, K. N.; Burant, J. C.; Millam, J. M.; Iyengar, S. S.; Tomasi, J.; Barone, V.; Mennucci, B.; Cossi, M.; Scalmani, G.; Rega, N.; Petersson, G. A.; Nakatsuji, H.; Hada, M.; Ehara, M.; Toyota, K.; Fukuda, R.; Hasegawa, J.; Ishida, M.; Nakajima, T.; Honda, Y.; Kitao, O.; Nakai, H.; Klene, M.; Li, X.; Knox, J. E.; Hratchian, H. P.; Cross, J. B.; Bakken, V.; Adamo, C.; Jaramillo, J.; Gomperts, R.; Stratmann, R. E.; Yazyev, O.; Austin, A. J.; Cammi, R.; Pomelli, C.; Ochterski, J. W.; Ayala, P. Y.; Morokuma, K.; Voth, G. A.; Salvador, P.; Dannenberg, J. J.; Zakrzewski, V. G.; Dapprich, S.; Daniels, A. D.; Strain, M. C.; Farkas, O.; Malick, D. K.; Rabuck, A. D.; Raghavachari, K.; Foresman, J. B.; Ortiz, J. V.; Cui, Q.; Baboul, A. G.; Clifford, S.; Cioslowski, J.; Stefanov, B. B.; Liu, G.; Liashenko, A.; Piskorz, P.; Komaromi, I.; Martin, R. L.; Fox, D. J.; Keith, T.; Al-Laham, M. A.; Peng, C. Y.; Nanayakkara, A.; Challacombe, M.; Gill, P. M. W.; Johnson, B.; Chen, W.; Wong, M. W.; Gonzalez, C.; Pople, J. A. *Gaussian 03*, revision B. 05; Gaussian, Inc.: Wallingford CT, 2004.
(32) Hay, P. J.; Wadt, W. R. *J. Chem. Phys*. **1985**, *82*, 270.
(33) Francl, M. M.; Petro, W. J.; Hehre, W. J.; Binkley, J. S.; Gordon, M.-H.; DeFree, D. J.; Pople, J. A. *J. Chem. Phys.* **1982**, *77*, 3654.
(34) Ghosh, A. *J. Chem. Phys.* **1997**, *101*, 3290−3297.
(35) Wondimagegn, T.; Ghosh, A. *J. Phys. Chem. B* **2000**, *104*, 10858−10862.
(36) Hay, P. J. *J. Phys. Chem. A* **2002**, *106*, 1634.
(37) Summers, J. S.; Stolzenberg, A. M. *J. Am. Chem. Soc*. **1993**, *115*, 10559−10567.
(38) Stratmann, R. E.; Scuseria, G. E.; Frisch, M. J. *J. Chem. Phys*. **1998**, *109*, 8128.
(39) Chiodo, S.; Russo, N.; Sicilia, E. *J. Comput. Chem*. **2005**, *26*, 175.
(40) Wachters, A. J. H. *J. Chem. Phys.* **1970**, *52*, 1033. Hay, P. J. *J. Chem. Phys.* **1977**, *66*, 4377.
(41) Barone, V.; Cossi, M. *J. Phys. Chem. A* **1998**, *102*, 1995.
(42) Cossi, M.; Barone, V. *J. Chem. Phys.* **2001**, *115*, 4708.
(43) Reed, A. E.; Curtiss, L. A.; Weinhold, F. *Chem. Rev*. **1988**, *88*, 899.
(44) Renner, M. W.; Fajer, J. *J. Biol. Inorg. Chem*. **2001**, *6*, 823−830.
(45) Stavrev, K.; Zerner, M. C. *Chem. Phys. Lett*. **1995**, *233*, 179−184.
(46) Spiro, T. G.; Kozlowski, P. M.; Zgierski, M. Z. *J. Raman Spectrosc*. **1998**, *29*, 869−879.
(47) Matsuzawa, N.; Ata, M. *J. Phys. Chem.* **1995**, *99*, 7698−7706.
(48) Zwaans, R.; van Lenthe, J. H.; den Boer, D. H. W. *J. Mol. Struct.* **1995**, *339*, 153−160.
(49) Zwaans, R.; van Lenthe, J. H.; den Boer, D. H. W. *J. Mol. Struct.* **1996**, *367*, 15−24.
(50) Goff, H.; La Mar, G. N.; Reed, C. A. *J. Am. Chem. Soc*. **1977**, *99*, 2026.
(51) Liao, M.-S.; Scheiner, S. *J. Chem. Phys*. **2002**, *117*, 205−219.
(52) Jensen, K. P.; Ryde, U. *ChemBioChem* **2003**, *4*, 413−424.
(53) Kozlowski, P. M.; Spiro, T. G.; Bérces, A.; Zgierski, M. Z. *J. Phys. Chem. B* **1998**, *102*, 2603−2608.
(54) Oliveira, K. M. T.; Trsic, M. *J. Mol. Struct.* **2001**, *539*, 107−117.
(55) Subramanian, J. In *Porphyrins and Metalloporphyrins*; Smith, K. M., Ed.; Elsevier Scientific: Amsterdam, The Netherlands, 1975; p 555.
(56) Lin, W. C. *Inorg. Chem*. **1976**, *15*, 1114.
(57) Scheidt, W. R. In *The Porphyrin Handbook*; Kadish, K. M., Smith, K. M., Guilard, R., Eds.; Academic Press: New York, 2000; Vol. 3, pp 49−112.
(58) Munro, O. Q.; Bradley, J. C.; Hancock, R. D.; Marques, H. M.; Marsicano, F.; Wade, P. W. *J. Am. Chem. Soc.* **1992**, *114*, 7218−7230.
(59) Barkigia, K. M.; Renner, M. W.; Furenlid, L. R.; Medforth, C. J.; Smith, K. M.; Fajer, J. *J. Am. Chem. Soc.* **1993**, *115*, 3627−3635.
(60) Collman, J. P.; Hoard, J. L.; Kim, N.; Lang, G.; Reed, C. A. *J. Am. Chem. Soc.* **1975**, *97*, 2676.
(61) Kutzler, F. W.; Swepston, P. N.; Berkovitch-Yellin, Z.; Ellis, D. E.; Ibers, J. A. *J. Am. Chem. Soc*. **1983**, *105*, 2996.
(62) Vasudevan, J.; Bumby, R. T.; Knapp, S.; Potenza, J. A.; Emge, T. J.; Schugar, H. J. *J. Am. Chem. Soc.* **1996**, *118*, 11676.
(63) Gouterman, M.; Wagniere, G. H.; Snyder, L. C. *J. Mol. Spectrosc.* **1963**, *11*, 108.
(64) Hashimoto, T.; Choe, Y. K.; Nakano, H.; Hirao, K. *J. Phys. Chem. A* **1999**, *103*, 1894.
(65) Adamo, C.; Scuseria, G. E.; Barone, V. *J. Chem. Phys*. **1999**, *111*, 2889−2899.
(66) Procyk, A. D.; Stolzenberg, A. M.; Bocian, D. F. *Inorg. Chem*. **1993**, *32*, 627−633.
(67) Hannah, S.; Lynch, V.; Guldi, D. M.; Gerasimchuk, N.; MacDonald, C. L. B.; Magda, D.; Sessler, J. L. *J. Am. Chem. Soc*. **2002**, *124*, 8416−8427.
(68) Improta, R.; Barone, V. *Chem Rev*. **2004**, *104*, 1231.
(69) Adamo, C.; Barone, V. *Chem. Phys. Lett*. **2000**, *330*, 152−160.
(70) Boys, S. F.; Bernardi, F. *Mol. Phys.* **1970**, *19*, 553.
(71) Barone, V.; Orlandini, L.; Adamo, C. *Chem. Phys. Lett*. **1994**, *231*, 295.